Lab on a Chip

PAPER

Microfluidic system for simultaneous optical measurement of platelet aggregation at multiple shear rates in whole blood†

Melissa Li,[a] David N. Ku[b] and Craig R. Forest[ab]

Thrombosis is the pathological formation of platelet aggregates which occlude blood flow causing stroke and heart attack–the leading causes of death in developed nations. Instrumentation for diagnosing and exploring treatments for pathological platelet aggregation thus has the potential for major clinical impact. Most current thrombosis methods focus on single flow conditions, non-occlusive platelet adhesion, or low shear rates and so are limited in their application to comparative studies involving multiple, pathological test conditions (*e.g.*, shear rate, stenotic geometries that mimic arteries, and rapid platelet accumulation to occlusion). The field could benefit from a low volume, high throughput, short analysis time, and low cost system while minimizing sample handling. We report on the design, fabrication, testing, and application of a microfluidic device and associated optical system for simultaneous measurement of platelet aggregation at multiple initial shear rates within four stenotic channels in label-free whole blood. Following computational design, requisite shear rates were achieved in the device by micro- surface milling a mold and subsequent PDMS casting. We applied the microfluidic system to measure platelet aggregation in whole porcine blood for shear rates spanning physiological to pathological flow conditions ($500–13000$ s^{-1}). Real-time, non-contact, label-free, microscope-free measurements of platelet aggregation were acquired using an optical system comprising a 650 nm diode laser and a linear CCD. We observed fully occlusive platelet aggregation in less than 20 min above a threshold initial shear rate of 4000 s^{-1}, and no occlusive platelet aggregation below 1500 s^{-1} ($N = 86$ trials). Accumulation of thrombus was consistent between laser intensity, light microscopy, histology, and mass flow rate measurements. The amount of blood volumes producing occlusion were dependent on shear rate. Times to occlusion were not found to be dependent on shear rate above the threshold level of 4000 s^{-1}. This microfluidic system enables measurement of the entire process of occlusive platelet thrombosis in whole, unlabeled blood, *in vitro*, at multiple shear rates. Such a system may be useful as a point-of-care diagnostic tool for studying anti-platelet therapies in individual blood samples from high-risk patients.

Introduction

Both biological and mechanical factors play primary roles in pathological, high shear platelet aggregation known as thrombosis–currently the leading cause of death in developed nations. Platelet aggregation has also been induced using external, soluable agonists.[1,2] Biological factors including vessel wall composition and cell surface changes have been relatively well characterized.[2–4] In contrast, the effects of mechanical factors including shear stress, hemodynamics, shear rate, and vessel morphology remain poorly characterized despite ample evidence of their influence. Platelets have long been known to aggregate in response to pathological shear rates exceeding 4000 s^{-1} in contrast to the mean physiological range estimated at $500–1500$ s^{-1}.[5,6] This behavior is significant because such elevated shear rates are commonly observed in clinical cases of coronary artery disease and atherosclerosis, conditions which affect more than 17 million Americans.[6–10] Furthermore, studies have shown the importance of locally constricted "stenotic" blood vessel morphologies in causing thrombosis using *in vivo*, *ex vivo* and *in vitro* models.[6,11,12] These experiments utilize single blood samples at single flow conditions, so comparative and comprehensive analyses are difficult to perform.

Measuring platelet aggregation using *in vitro* devices has been challenging. The formation of a thrombus occurs in three phases: (I) initial adhesion of platelets to a substrate, (II) the rapid accumulation of platelets binding to other platelets and (III) the

[a]Department of Biomedical Engineering, Institute for Bioengineering and Biosciences, Room 2103, 315 Ferst Drive, Atlanta, GA, USA. E-mail: melissa_li@gatech.edu; Tel: +1 404 385 7645
[b]Department of Mechanical Engineering, Georgia Institute of Technology, 815 Ferst Drive, Atlanta, GA, USA
† Electronic supplementary information (ESI) available. See DOI: 10.1039/c2lc21145a

final stabilization and contraction of the platelets into a solid mass that occludes flow.[5,6] Many studies are often conducted only on the initial adhesion phase[7,8] using fluorescence microscopy and are not well suited to volumetric measurements in real time. Microscopy methods are limited by small measurement areas, poor depth measurement, the need for image post-processing, and often require sample pre-treatment.

Recently, Gutierrez et al.[13] showed the importance of platelet receptor integrin αIIbβ3 in genetically modified mice platelets' adherence to collagen (thrombosis phase I) at low shear rates 50–1410 s^{-1} in a multichannel microfluidic device. While this device was able to address multiple shear rates in multiple channels simultaneously, these tests did not include pathologically relevant high shear behavior or rapid platelet accumulation (thrombosis phase II).[14] Other recent work by Tovar-Lopez et al.[12] has shown the importance of stenotic geometry to high-shear platelet aggregation using microscale devices. While this study and device thoroughly analyzed changes in platelet aggregation downstream of the stenosis, it did not examine aggregation within the stenoses nor explore aggregation at varying shear rates in identical stenoses.

Thus current methods have been limited by one or more of the following parameters: limited relevance to physiological flow,[15,16] need for external cell labeling,[13,17–19] platelet fractionation and washing for imaging and analysis,[20,21] non-pathologically relevant low shear rates,[4,6,7] small measurement area limited by microscopy,[2,6,7] channel sizes insufficient to observe rapid platelet accumulation, and large volumes of blood.[22] Additionally, many in vitro models have not attempted to address aspects of specific clinical pathologies relevant to thrombosis including high shear rates and stenotic morphology.[1,5–7] Commercialized methods for platelet function analysis are able to perform testing on single samples at a single shear rate under flow conditions–including high speed bead mixing, forced flow through a membrane, cone-and-plate flow–which are not relevant to biological flow through blood vessels and have shown inconclusive results.[16,23]

Clinically, anti-platelet agent dosing is a persistent medical challenge (e.g., 5–14% of patients are unresponsive to prescribed therapies),[24] and their effects are suspected to be shear rate dependent.[25] By testing patients' blood in the device and comparing the occlusion times at a range of shear rates between a dosed and control cohort such as the one presented here, we anticipate point-of-care assessment of the efficacy of the patient drug dosage.

There is presently no instrumentation able to simultaneously examine individual trials of a wide range of fluid shear rates including those exceeding 10000 s^{-1}, with simultaneous platelet aggregation to occlusion measurement, which is important given the time dependent effects of clotting and anticoagulants. The creation and application of such high throughput instruments could enable essential, large scale, comprehensive studies which would inform research on cardiovascular pathologies and their appropriate anti-platelet therapies.

In this study, we report on the design, fabrication, testing, and application of a microfluidic device for inducing platelet aggregation to full occlusion within four microfluidic stenotic channels in label free whole blood. The stenotic channel geometry mimics the arterial profiles found in clinical pathology, enables high local shear rates, and enables shear gradients that have been shown to be important in thrombosis.[11] An associated optical system enables measurement of this aggregation to occlusion using a microscope-free, multi-channel, label-free, real-time method based on difference in optical properties between platelets and red blood cells.

Following fluid and optical modeling, we designed and fabricated the four channel microfluidic device and laser optical system. Performance of the microfluidic system was first verified by experiments showing that platelet-rich thrombi were formed and measurable within the stenotic high shear regions using optical microscopy and histology. We applied our system to measure time (∼10 min) and volume (∼5 mL) to occlusion for 108 channel runs among 14 porcine samples at varying shear rates.

Methods

The microfluidic system design and operation are shown in Fig. 1. The device enables formation of thrombi at four distinct initial shear rates between 500 and 13000 s^{-1} from a constant pressure source within corresponding stenotic regions of the branching channels intended to mimic coronary arteries.

An associated optical system for measuring platelet aggregation measures an increase in light transmission as the platelets aggregate in the four stenotic regions during shear-mediated thrombosis. The integration and operation of this optical system
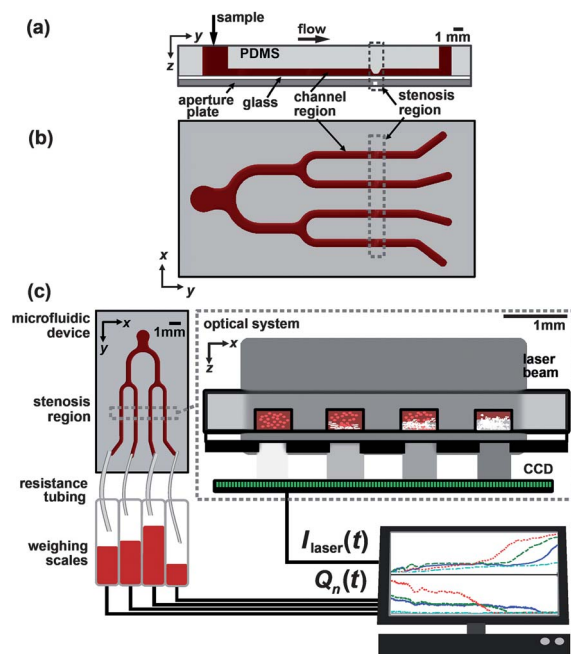
Fig. 1 Schematic showing (a) side and (b) top view of the design of the microfluidic device for inducing platelet aggregation at four distinct initial shear rates in whole blood within the high shear stenotic regions. (c) The microfluidic system comprises the microfluidic device and optical system. The optical system measures an increase in light transmission (from the laser to the CCD), $I_{laser}(t)$, as the platelet aggregation in the stenotic regions increases during shear-mediated thrombosis. The shear rates in each stenotic region are controlled by resistance tubing, which terminates in independent weighing scales to measure flow rates $Q_n(t)$.

with the microfluidic device are shown in Fig. 1c. To compare the performance of our laser optical system to conventional microscopy, we time-multiplexed the two during the same experiment using an electrical relay while measuring flow rate. Outlet tubing of various lengths and diameters is used to induce initial shear rates and these tubes terminate in separate, independent weighing scales to measure volumetric flow rate.

Device design and fluid modeling

The device was designed to address shear rates of 500, 1500, 4000, 7000, 10000, and 13000 s^{-1} within the channels' high-shear stenotic regions. These shear rates were chosen to represent the physiological shear rate range (500–1500 s^{-1}), pathological shear rates (4000 s^{-1}), and high pathological shear rates (10000 s^{-1} and above)—all discussed in the introduction. We obtained a set of four of these six shear rates during a single experiment within the branching channels from a common pressure difference of 1400 Pa. In contast to contant volumetric flow rate, constant pressure-driven flow seems preferable for the measurement of thrombus growth to full occlusion; as the thrombus reaches full occlusion, contant volumetric flow rate requires large velocities that can cause non-physiologically relevant high forces on the growing platelet thrombus. Blood viscosity, μ, and density, ρ, were assumed constant (valid for shear rate $\dot{\gamma} > 6$ s^{-1} [26]) at 0.00385 Pa·s and 1.080 g mL^{-1}, respectively. As a design consideration, while other work [11,13] has limited the minimum channel dimension to 20–50 μm; we chose a minimum dimension of 250 μm to enable observation of rapid platelet accumulation, for comparison with prior work. [14] Another consideration was the design of the stenosis to reflect pathologically relevant geometry. Thus we designed the diameter reduction from the channel region to the stenosis region to be 53%, near to the 50% reduction often used as an indicator for surgical intervention in the left main coronary artery. [27] In the channels upstream and downstream of the high-shear stenotic regions, we require that the maximum shear rates not exceed 1500 s^{-1}, the upper bound of physiological shear rates.

In order to obtain a wide range of shear rates in multiple identical microchannels sharing a single flow input, we passively controlled channel flow resistance downstream of the stenotic region through the use of Tygon tubing (Saint Gobain, 50SHL). Thus our finite volume fluid modeling efforts combined the effects of the channel and tubing resistances. While other groups have used on-chip resistive channels for controlling flow rates, [13] this off-chip resistive tubing design enables simple shear rate control over two orders of magnitude from an array of identical microchannels, simplifies fabrication, and interfaces easily with weighing scales for flow rate measurement (See Fig. 2).

To determine shear rate distribution, design the channel geometry, and select resistance tubing, we performed finite volume fluid modeling using ANSYS (Ansys Inc., Canonsburg, PA). Modeling was performed using a mesh with volume size of 2 μm minimum side length within the stenosis to approximate the boundary layer region in which a platelet (2–20 μm diameter) binds. Previously mentioned input pressure, viscosity, and density were used to determine shear rate distribution as a function of channel and tubing dimensions. We applied this model to select resistive tubing ranging from $L = 0.6$ m, $d = 0.8$ mm to $L = 0.3$ m, $d = 2.4$ mm.
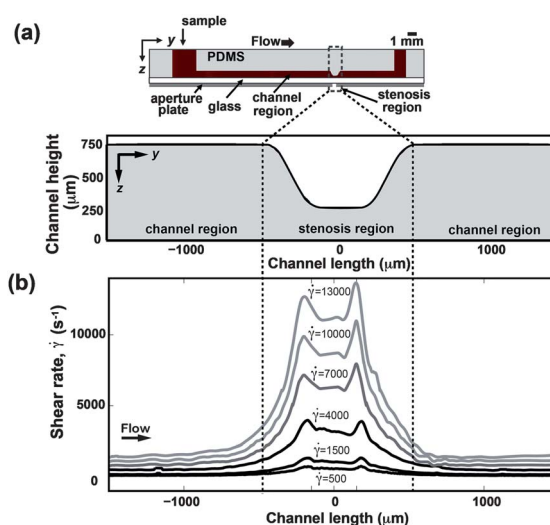
Fig. 2 Six shear rate profiles were computed and were obtained experimentally by varying outlet tubing geometry connected to a uniform channel geometry (a). The maximum shear rate outside of the stenoses regions is within physiological range <1500 s^{-1}, while maximum shear rate within the stenoses were designed for a variety of physiological and pathological shear rates (500–13000 s^{-1}) (b).

Device fabrication

Traditional semiconductor fabrication methods are commonly limited to hydraulic diameters of 5–200 μm and relatively large effort is necessary to obtain curved, three-dimensional topographies. Thus, in order to fabricate a microfluidic device with the requisite change in hydraulic diameters (300–1000 μm) as well as the gradual transition to the stenosis from the non-stenotic channel region (See Fig. 4), we utilized an unconventional microfabrication technique. We first created a mold in aluminum 6013 using a vertical milling machine (Haas, OM-1a, Oxnard, CA). The milling process used square endmills with diameters $D = 0.25$–1.57 mm and a ball endmill with $D = 125$ μm operated at a spindle speed of 30,000 rpm. For all tools, feed rates were 50.8 mm min^{-1}; depths of cut were D/3. Unattended mold machining time was approximately 30 h, attended user- operation time was approximately 2 h. Mold surface average roughness, Ra, measured by white light interferometry (Zygo, NewView 200, Middlefield, CT), was approximately 150 nm, less than the 2 μm platelet diameter, and so was deemed sufficient.

From this mold, we cast the poly-dimethylsiloxane (PDMS) device layer and bonded it to glass slide following plasma gas exposure (Harrick Plasma, Ithaca, NY) to form enclosed channels. Enclosed channels were filled with collagen I (Sigma Chemicals, St. Louis, MO) to initiate platelet surface adhesion and allowed to incubate overnight. [2,7] The aluminum mold has been used at least 100 times without performance degradation.

Light transmission through platelet thrombus

To design a laser optical system to measure platelet aggregation, we applied a Monte Carlo radiative transport optical modeling tool [28] capable of accounting for the inherent stochastic scattering and absorption of light in blood.

The transmission of light through blood's components varies. Platelets are less scattering and less absorbing to visible light (250–850 nm) than red blood cells due to differences in their index of refraction and lack of hemoglobin.[29] Therefore, as platelet-rich thrombus accumulates in the stenosis, otherwise filled with blood, light transmitted through it increases.

The Monte Carlo optical model accounts for the wavelength dependent scattering coefficient, α_s, absorption coefficient, α_a, anisotropy of scattering, g, and refractive index, n of both the platelet thrombus and whole blood (hematocrit, Hct = 0.41). Previous work[29] has measured and tabulated these parameters for whole blood and diffuse concentrations of platelets, but we require α_s for platelet-rich thrombus rather than diffuse platelets in saline. Accordingly, we utilized a published confocal reflectance technique[30–32] after confirming its accuracy by measuring known α_s for Intralipid-20 1% v/v (Sigma-Aldrich, St. Louis, MO).[33] Measurements were performed on occlusive platelet thrombi, within two hours of formation. Platelets were labelled with the fluorophore mepacrine to ensure scattering measurements were acquired in the correct location. Mepacrine's 525 nm emission was spectrally excluded from the platelet aggregation measurement wavelength bandpass and its low concentration (<1%) minimized scatting effects. Mepacrine was not used in any other experiments.

The laser optical system used for measuring platelet aggregation comprises a 650 nm, 0.9 mW (CVI Melles Griot, Albuquerque, NM) laser diode, spatially filtered, along with a 3000 pixel 12-bit linear CCD with pixel dimensions 7 μm × 200 μm (Thorlabs, LC1 USB, Newton NJ), depicted in Fig. 2. Optical cross-talk between channels is mitigated with sufficient channel spacing and the use of an aperture plate (See Fig. 1, 2), made from laser-cut, toner-coated polyester. The aperture plate is aligned and glued to the bottom of each sealed device.

Experimental protocol

Porcine blood samples obtained fresh from a local abattoir were treated immediately with 3.5 Units/mL of unfractionated porcine heparin (Elkins-Sinn Inc., Cherry Hill, NJ) and were used within five hours of collection. This concentration of heparin has been used by others to prevent clotting in storage reservoirs while allowing thrombus formation under flowing conditions.[14] In contrast, the more widely used citrate requires the addition of ADP to re-activate platelets after its addition.[9,34] Blood samples were prevented from sedimenting by rotation on a laboratory shaker at about 60 rpm. Prior to experiments, the blood was filtered by flowing it slowly through a 200 μm pore polypropylene mesh (Smallparts, Seattle WA) to remove platelet or lipid aggregates that could cause embolic occlusion. To verify the platelet composition of the occlusive thrombus, we used Carstairs histological staining method.[18] To perform Carstairs staining, we excised the PDMS layer containing attached thrombi, preseved them with formalin for 48 h, dehydrated them in a series of xylene washes, fixed them in paraffin, microtome sectioned them into 5 μm slices, and stained them. The stain colors platelets blue and red blood cells orange/red. Thrombus volume within the stenosis was estimated by multiplying its cross-sectional area by the height of the stenosis.

Devices were primed with a mixture of 43% glycerol/phospate buffered saline (Sigma Chemical, St. Louis, MO), viscosity matched at μ = 0.00385 Pa·s prior to flowing blood. Glycerol and blood were pressurized to 1400 Pa for flow into the device with an open, suspended syringe with 132 mm of gravity pressure head. This pressure head was maintained during the course of an experiment with by visually observing changing fluid reservoir height and adding additional fluid with a syringe as neccesary, resulting in a pressure uncertainty of ~30 Pa. The volumetric flow rates were compared between modeled flows, a glycerol solution, and highly heparinized blood (35 Units/mL) to evaluate modeling accuracy.

The microfluidic device was aligned to the laser optical system and microscope using a 3-axis translation stage. Laser intensity transmitted through each of the four stenosis regions, $I_{laser}(t)$, was recorded and flow rate, $Q_n(t)$, was measured by weighing scales with 0.01 g resolution placed at the outlet of each channel n (Adam Equipment, Danbury, CT), according to $Q = \Delta m/\rho\Delta t$, where m is mass and ρ is density. White-light microscopy images were acquired with a Zeiss Stemi 2000c microscope under 5.0X magnification and a Motic 2000 CCD camera in a detection method used by others.[14] Hardware control and acquisition were sampled at 1 Hz with 20 ms integration time using Labview (National Instruments, Austin TX) and data was analyzed using Matlab (Mathworks, Natick, MA). Optical measurements were normalized as $[I(t) - I_{min}]/I_{max}$ and low-pass filtered to produce relative intensity measurements $I_{microscope}(t)$ and $I_{laser}(t)$.

Results and discussion

We first compared modeled and experimental flow rates within the microfluidic device. Next, we verfied that our system was able to form occlusive platelet aggregates. We then used our optical model to design and validate the optical system for measuring platelet aggregation and sensing occlusion. Finally, we tested ability of the integrated microfluidic system to form and measure platelet aggregation to occlusion in parallel with microscopy and flow-based measurements. We then applied our system to measure time and volume to occlusion 108 channel runs amongst 14 porcine samples at varying shear rates and confirmed the formation of platelet-rich thrombi in the channels by histology.
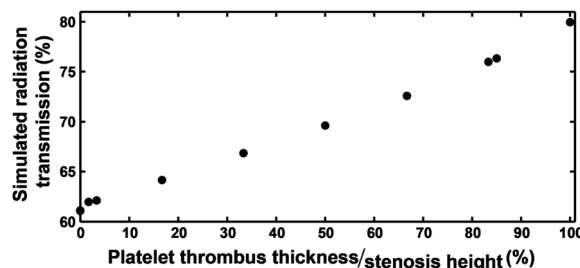
Fig. 3 Monte Carlo simulated relationship of the percentage of 633 nm light transmitted through a platelet thrombus of varying thicknesses within a 250 μm stenosis filled with blood. Light transmitted is predicted to increase by 19% from whole blood (0%) to fully occlusive thrombus (100%).

Fluid modeling

Computational fluid dynamics (ANSYS) was used to quaantify shear rate in the test section, shown in Fig. 3. The maximum shear rate upstream and downstream of the stenosis region is <1500 s^{-1}, within the physiological range of normal arterial flow. Shear rates were calculated as the average wall shear rate along x-z cross sections. Observing the distribution of shear rates along the channel length reveals the highest shear rate at the entrance of the stenosis, where we expect initiation of platlet aggregation, both of which others have reported.[6] Flow was laminar with Re = 3–27. Additionally, this modeling revealed that a gradual cross-sectional area transition to the stenosis from the non-stenosis channel region, as shown in Fig. 3a, reduces flow velocity variation as compared with an abrupt transition, more accurately mimicking physiological conditions and prior in vitro work.[6]

Adhered and aggregated platelets reduce the stenosis diameter and correspondingly change the wall shear rate. Applying our fluid modeling, we estimate an exponential increase in shear rate as a function of decreasing cross-sectional area, up to a maximum (2–4 times initial wall shear rate for all shear rates and pressure in this study), after which it rapidly falls to zero.

Measured flow rates are compared with modeled flow rates in Table 1. Post-testing microscopy did not show any accumulated platelet mass from the blood flow, as expected.

Thrombus histology

Thrombus histology results using Carstairs staining method (See Supp. Fig. 1†) indicate that thrombi formed within the stenosis region of our devices showed high concentrations of platelets with low concentrations of fibrin at high shear rates and red blood cell-rich thrombi at low shear rates, as expected and consistent with previous reports.[8,9] Volumes of thrombi were estimated at 0.0256 µL (N = 7), approximately 55% of the stenosis volume.

Optical modeling

The experimentally determined scattering coefficient for platelet thrombus is shown along with published optical properties of whole blood and platelets in Table 2 (α_s = 184–203 for N = 3).

Using the Monte Carlo optical model with the properties of Table 2, we calculated the expected increase in transmitted light

Table 1 Modeled and experimentally verified steady flow rates in the microfluidic device. For both glycerol and heparinized blood, flow rates match the model well at all shear rates well. Measured flow rates are shown as averages ± standard deviation. Instrument (weighing scale) measurement uncertainty is 0.3 µL s^{-1}

Shear rate, $\dot{\gamma}$ (s^{-1})	Q_{model} (µL s^{-1})	$Q_{glycerol}$ (µL s^{-1})	Q_{blood} (µL s^{-1})
500	1	0.5 ± 0.4	0.6 ± 0.3
1500	5	3 ± 1	3 ± 1
4000	15	13 ± 1	13 ± 1
7000	19	17 ± 1	17 ± 1
10000	24	27 ± 2	27 ± 2
13000	40	39 ± 7	39 ± 3

Table 2 Cited and measured optical properties (scattering coefficient, α_s; refractive index, n; absorption coefficient, α_a; anisotropy of scattering, g) for whole blood and platelet thrombus at 633 nm

Sample	α_s (cm^{-1})	n	α_a (cm^{-1})	g
Blood, Hct 0.41	794[b]	1.42[b]	7.92[b]	0.99[b]
Platelet thrombus	**193**[a]	1.35[b]	1.21[b]	0.96[b]

[a] Measured in this work. [b] Cited from published data.[29]

intensity as a function of platelet thrombus thickness within the channel. The results (See Fig. 3) show a linear increase, up to a 19% change in light transmitted at full occlusion in which the thrombus thickess equals the full channel stenosis height. These results are supported by experimental results, which show increases in absolute light intensity of 24 ± 10.2% (N = 68) for a thrombus whose thickness spans the entire stenosis height.

Platelet aggregation measurements

We first used the microfludic system to form and detect platelet aggregation to full occlusion of flow at 10000 s^{-1} initial shear rate with simultaneous optical (microscope and laser optical system) and flow rate measurements. Results of a typical experiment are shown in Fig. 4. From the time series of raw microscope images of platelets aggregating in the stenosis (Fig. 4a), normalized intensity, $I_{microscope}(t)$, was computed for comparison with the laser optical system intensity transmitted, $I_{laser}(t)$ (Fig. 4b). Occlusion times between the methods differ by 3.97% ± 5.1% (N = 6) with Pearson product-moment correlation coefficient, or Pearson's r, of 0.94, p < 0.01. Both optical methods show rapid platelet accumulation (Fig. 4).[6,8,22,35]

The flow rate measurements, $Q(t)$, shown in Fig. 4b, also show the occlusion time. From this flow rate measurement, we were able to calibrate the intensity at which occlusion occurs in the laser optical system by setting a threshold as a percentage of maximum intensity. Flow rate is nearly constant while platelets accumulate in the stenosis because the stenosis is a small fraction of the overall resistance of the microfluidic channel and associated resistance tubing. From our fluid modeling, we estimate that the resistance of the stenosis reaches the same order of magnitude
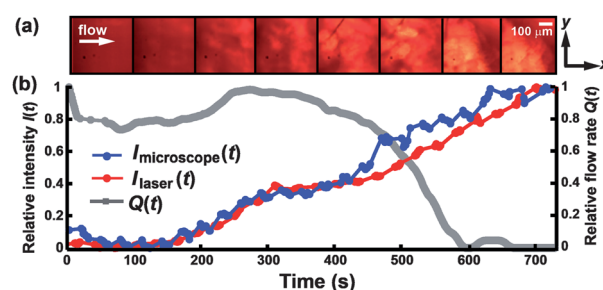
Fig. 4 (a,b) Formation and measurement of platelet aggregation to full occlusion of flow in the microfluidic device using simultaneous measurements of microscope intensity, $I_{microscope}(t)$; light transmission, $I_{laser}(t)$; and flow rate, $Q(t)$, at 10000 s^{-1} initial shear rate. Microscope images (a) show aggregation–brighter areas of the images correspond to more platelet mass. The correlation between microscope intensity and light transmission measurements was calculated as Pearson's r = 0.94.

as the rest of the system at 28% occlusion, at which point (~400 s), the flow rate begins to decay logarithmically, as confirmed by our fluid modeling efforts (not shown).

Next, we applied the microfluidic system to whole porcine blood for shear rates spanning physiological to pathological flow conditions. For each porcine blood sample, four shear rates were run simultaneously in a single trial while platelet aggregation to occlusion was measured by the laser optical system only and flow rates were measured by the weighing scales. A trial is defined as a single experiment with one new microfluidic device comprising four channel runs. Up to three trials were run with each sample.

In total, 14 porcine blood samples were run on a total of 27 trials resulting in N = 4 channels/device × 27 trials = 108 channel runs. Of these samples, 5/14 (36%) showed no occlusion at any shear rate or showed emboli at all shear rates, so these were excluded after a single trial. Embolus was defined as decrease in flow rate to less than 50% of initial within 30 s.[14] Of the remaining 9 samples run in 22 trials (N = 88 channel runs), none of the channels with initial shear rate of 500 s^{-1} and 1500 s^{-1} formed occlusive thrombi over 2000 s (N = 18). This finding is consistent with previous work which has shown that rapid platelet accumulation is absent with low shear rates (<2000 s^{-1}).[14] The other N = 70 channels were run at a variety of higher shear rates. Only two high-shear experiments did not clot (one at 4000 s^{-1}, one at 7000 s^{-1}), while in the other rest, occlusive thrombi formed at times less than 1200 s (N = 68). This finding is consistent with reports from others that the platelet protein vWF begin to show significantly adhesive action at shear rates of 4000 s^{-1}.[36] The times to occlusion for the N = 68 channel runs

described are shown in Fig. 5a, along with the corresponding standard deviations. The average difference between the optical and flow rate measurement of time to occlusion was 8.4%; the standard deviations of the time to occlusion measurements ranged from 50–212 s. For this range of pathological shear rates (4000–13000 s^{-1}), we did not observe a statistically significant (p < 0.05) difference in the time to occlusion *versus* shear rate. Our findings with N = 86 channel runs suggest that thrombosis is binary, present above 4000 s^{-1} and not present below 1500 s^{-1}. We have not studied this transition regime at higher resolution in this work.

To examine the *intra*-trial variability of blood clotting behavior, we measured how the blood clotting behavior varies between adjacent chanels in the same trial with the same blood on the same device at the same shear rate. In 14 trials with duplicate shear rates channel runs (D = 14 sets), we measured the average standard deviation of the clotting time, σ, for the sets. The average across all shear rates (D = 14) was σ = 75 s. The average at specific shear rates was, for $\dot{\gamma}$ = 4000 s^{-1}, σ = 30 s (D = 2); for $\dot{\gamma}$ = 7000 s^{-1}, σ = 99 s (D = 9); and for $\dot{\gamma}$ = 10000 s^{-1}, σ = 34 s (D = 3)). To study the *inter*-trial variability, we measured how the blood clotting behavior varies between succesive trials with the same blood at the same shear rate, we ran 9 triplicate channel runs (T = 9 sets) and computed the average standard deviation of the clotting times for the sets. The average across all shear rates (T = 9) was σ = 106 s. The average at specific shear rates was, for $\dot{\gamma}$ = 7000 s^{-1}, σ = 155 s (T = 3); for $\dot{\gamma}$ = 10000 s^{-1}, σ = 61 s (T = 2); and for $\dot{\gamma}$ = 13000 s^{-1}, σ = 91 s (T = 4)). Since the intra- and inter-trial variability measured were similar, occlusion time measurements across different trials and channels at common shear rates were comparable.

Similarly, the volume, V, of blood required to form occlusive thrombus at each shear rate are determined (V = m/ρ), shown in Fig. 5b. The volume required are significantly different (p < 0.05), save the 7000 s^{-1} to 10000 s^{-1} comparison.

Previous reports on shear-dependent platelet aggregation have shown mixed results, with some reporting increases in platelet growth rates at shear rates in excess of 7000 s^{-1} and others reporting no increases.[37] In contrast to all previous methods, we have measured occlusion time at these high shear rates *simultaneously* and report no significant change in occlusion time in excess of 4000 s^{-1}, and hence platelet growth rate. Potentially, the use of a syringe pump used by others, rather than constant pressure we have used, exposes platelets to non-physiologically high pressure forces during the late stages of occlusion.

Fig. 5 (a) Shear rates *vs.* occlusion times for six initial shear rates measured using the optical system and flow rate. Error bars indicate one standard deviation. For the range of pathologically relevant shear rates (4000–13000 s^{-1}), we did not observe a statistically significant (p < 0.05) difference in the time to occlusion *versus* shear rate. (b) Shear rate *vs.* volume of blood required to occlude flow. Error bars indicate one standard deviation. We observed statistically significant (p < 0.05) differences in the volume to occlusion *versus* shear rate, save the 7000 s^{-1} to 10000 s^{-1} comparison.

Conclusions

High shear rate platelet aggregation is central to the study of thrombosis. To study the effects of shear rate, we developed a multi-channel optical *in vitro* method to simultaneously characterize changes in the times and volumes to platelet-based occlusive thrombus formation in whole, label-free blood samples across multiple shear rates over both the physiological pathological range. The use of a laser to quantify thrombosis growth in whole, label-free blood is faster and simpler than fractionation and microscopy techniques.[13,17,38] For example, mepacrine staining requires low shear mixing and fluorescence imaging. This four channel throughput enables direct comparison, in

parallel, of the effects of shear rate independent of potentially confounding factors such as sample age, variations in sample handling, anticoagulant concentration, and channel geometry unlike previous serial studies.[37,39]

Our findings suggest that shear-dependent occlusion time from thrombosis is binary, present above 4000 s^{-1} and not present below 1500 s^{-1}. We did not observe a statistically significant (p < 0.05) difference in the time to occlusion *versus* shear rate. Intra- and inter-trial variability were similar, so occlusion time measurements across different trials and channels at common shear rates are comparable. In contrast, the blood volumes required for flow to full occlusion are significantly different (p < 0.05), save the 7000 s^{-1} to 10000 s^{-1} comparison.

Fluid modeling was developed for the four channel micro-fluidic device design and used to compute flow rates, which were experimentally verified. Optical modeling revealed expected, and subsequently verified, increases in light transmitted through the stenoses as platelets aggregate. Analysis using microscopy and histology reveal that platelet-rich occlusive thrombi form above 4000 s^{-1}, consistent with previous reports,[6,9,11] thus validating its use in platelet aggregation studies.

Using micromilling for device mold fabrication enables precise control over channel geometry in the range of 250–2500 μm. Compared to semiconductor fabrication processes, micromilling permits tapered stenosis channel profiles with reduced edge-induced flow effects. It also requires less capital equipment and enables shorter design cycles. While this fabrication method and collagen coating method (rather than a combination of ADP or epinephrine to artificially induce platelet activation and accelerate thrombus formation[34]) enables channels of sufficient size and adhesion for formation and measurement of thrombus growth to full occlusion, respectively, these channels *do* require a larger blood volume per channel, 2–8 mL, in contrast to the 0.8 mL used by others.[16] Regarding a potential compliance mismatch between our PDMS flow channels and arteries, several groups have previously shown that vessel compliance has a minor effect on wall shear stress that would be dwarfed by the shear effect of thrombosis narrowing the lumen.[6,40–43] Further, reported Young's Moduli are comparable (*e.g.*, PDMS elasticity = 0.38–0.75 MPa,[44] human vessels elasticity at physiological blood pressure = 0.5–2 MPa[45–47]).

The laser optical system described should be scalable to tens to hundreds of channels whereas the conventional microscope and flow rate measurements, which yield similar occlusion times are typically limited to single channels. Measurements of occlusion from our optical system showed high correlation (r = 0.94) compared with more expensive and bulky white light microscopy methods, and it is potentially more easily miniaturized. Future work will apply this microfludic device and laser optical system to the clinical characterization of patient blood clotting with and without anti-platelet agents at varying shear rates, since these agents' efficacy is suspected to be shear rate dependent.

We have presented a proof of concept for applying clinically derived pathological flow conditions to whole blood samples in a microscope-free, high throughput, microscale system. In contrast to current clinical platelet diagnostics including parallel plate assays and commercial devices,[25] our system is able to examine platelet activity under multiple, well-defined shear flow conditions simultaneously at volumes consistent with typical clinical blood draws.

Notes and references

1 G. Dangas, J. J. Badimon and B. S. Coller, *et al.* Administration of abciximab during percutaneous coronary intervention reduces both ex vivo platelet thrombus formation and fibrin deposition - Implications for a potential anticoagulant effect of abciximab, *Arterioscler., Thromb., Vasc. Biol.*, 1998, **18**(8), 1342–1349.

2 B. Lincoln GM, A. J. Ricco and LPL. Analysis of whole blood platelet translocation on a vWF-coated microfluidic flow chamber. In: *12th International Conference on Miniaturized Systems for Chemistry and Life Sciences (μTAS2008)*. San Diego, CA; 2008:453–455.

3 B. Savage, E. Saldívar and Z. M. Ruggeri, Initiation of platelet adhesion by arrest onto fibrinogen or translocation on von Willebrand Factor, *Cell*, 1996, **84**(2), 289–297.

4 B. Savage, F. Almus-Jacobs and Z. M. Ruggeri, Specific synergy of multiple substrate–receptor interactions in platelet thrombus formation under flow, *Cell*, 1998, **94**(5), 657–666.

5 Z. M. Ruggeri, Platelets in atherothrombosis, *Nat. Med.*, 2002, **8**(11), 1227–1234.

6 D. M. Wootton and D. N. Ku, Fluid mechanics of vascular systems, diseases, and thrombosis, *Annu. Rev. Biomed. Eng.*, 1999, **1**, 299–329.

7 Z. M. Ruggeri, J. N. Orje, R. Habermann, A. B. Federici and A. J. Reininger, Activation-independent platelet adhesion and aggregation under elevated shear stress, *Blood*, 2006, **108**(6), 1903–1910.

8 M. J. Maxwell, E. Westein and W. S. Nesbitt, *et al.* Identification of a 2-stage platelet aggregation process mediating shear-dependent thrombus formation, *Blood*, 2007, **109**(2), 566–576.

9 L. Badimon Influence of arterial damage and wall shear rate on platelet deposition. Ex vivo study in a swine model. *Arterioscler Thromb Vasc Biol.* **6**(3):pp. 312–320.

10 V. T. Turitto and C. L. Hall, Mechanical factors affecting hemostasis and thrombosis, *Thromb. Res.*, 1998, **92**(6 Suppl. 2), S25–31.

11 W. S. Nesbitt, E. Westein and F. J. Tovar-Lopez, *et al.* A shear gradient-dependent platelet aggregation mechanism drives thrombus formation, *Nat. Med.*, 2009, **15**(6), 665–673.

12 F. J. Tovar-Lopez, G. Rosengarten and E. Westein, *et al.* A microfluidics device to monitor platelet aggregation dynamics in response to strain rate micro-gradients in flowing blood, *Lab Chip*, 2010, **10**, 291.

13 E. Gutierrez, B. G. Petrich and S. J. Shattil, *et al.* Microfluidic devices for studies of shear-dependent platelet adhesion, *Lab Chip*, 2008, **8**(9), 1486.

14 A. Para, D. Bark, A. Lin and D. Ku, Rapid Platelet Accumulation Leading to Thrombotic Occlusion, *Ann. Biomed. Eng.*, 2011, **39**(7), 1961–1971.

15 S. K. Kundu, T. S. Geiselman *Method for testing coagulation of blood through bioactive porous partition members*. 1998.

16 C. K. Hofer, A. Zollinger and M. T. Ganter, Perioperative assessment of platelet function in patients under antiplatelet therapy, *Expert Rev. Med. Devices*, 2010, **7**(5), 625–637.

17 K. B. Neeves and S. L. Diamond, A membrane-based microfluidic device for controlling the flux of platelet agonists into flowing blood, *Lab Chip*, 2008, **8**(5), 701–709.

18 K. B. Neeves, S. F. Maloney and K. P. Fong, *et al.* Microfluidic focal thrombosis model for measuring murine platelet deposition and stability: PAR4 signaling enhances shear-resistance of platelet aggregates, *J. Thromb. Haemostasis*, 2008, **6**(12), 2193–2201.

19 F. Shen, C. J. Kastrup, Y. Liu and R. F. Ismagilov, Threshold response of initiation of blood coagulation by tissue factor in patterned microfluidic capillaries is controlled by shear rate, *Arterioscler., Thromb., Vasc. Biol.*, 2008, **28**(11), 2035–2041.

20 B. Linnemann, J. Schwonberg, H. Mani, S. Prochnow and E. Lindhoff-Last, Standardization of light transmittance aggregometry for monitoring antiplatelet therapy: an adjustment for platelet count is not necessary, *J. Thromb. Haemostasis*, 2008, **6**(4), 677–683.

21 C. P. M. Hayward, M. Pai and Y. Liu, *et al.* Diagnostic utility of light transmission platelet aggregometry: results from a prospective study of individuals referred for bleeding disorder assessments, *J. Thromb. Haemostasis*, 2009, **7**(4), 676–684.

22 D. M. Wootton, C. P. Markou, S. R. Hanson and D. N. Ku, A mechanistic model of acute platelet accumulation in thrombogenic stenoses, *Ann. Biomed. Eng.*, 2001, **29**(4), 321–329.

23 A. D. Michelson, A. L. Frelinger and M. I. Furman, Current options in platelet function testing, *Am. J. Cardiol.*, 2006, **98**(10), 4N–10N.

24 Center for Drug Evaluation and Research. Postmarket Drug Safety Information for Patients and Providers - FDA Drug Safety Communication: Reduced effectiveness of Plavix (clopidogrel) in patients who are poor metabolizers of the drug. Available at: http://www.fda.gov/Drugs/DrugSafety/PostmarketDrugSafetyInformationforPatientsandProviders/ucm203888.htm. Accessed March 29, 2011.

25 J. J. Zwaginga, K. S. Sakariassen and G. Nash, *et al.* Flow-based assays for global assessment of hemostasis. Part 2: current methods and considerations for the future, *J. Thromb. Haemostasis*, 2006, **4**(12), 2716–2717.

26 G. P. Galdi, R. Rannacher, A. M. Robertson and S. Turek, Hemodynamical flows: modeling, analysis and simulation, *Birkhäuser*, 2008.

27 D. Ku, Blood flow in arteries, *Annu. Rev. Fluid Mech.*, 1997, **29**, 399–434.

28 L. Wang, S. L. Jacques and L. Zheng, MCML–Monte Carlo modeling of light transport in multi-layered tissues, *Comput. Methods Programs Biomed.*, 1995, **47**(2), 131–146.

29 M. Meinke, G. Muller, J. Helfmann and M. Friebel, Optical properties of platelets and blood plasma and their influence on the optical behavior of whole blood in the visible to near infrared wavelength range, *J. Biomed. Opt.*, 2007, **12**(1), 014024–9.

30 T. Collier, D. Arifler, A. Malpica, M. Follen and R. Richards-Kortum, Determination of epithelial tissue scattering coefficient using confocal microscopy, *IEEE J. Sel. Top. Quantum Electron.*, 2003, **9**(2), 307–313.

31 R. A. Drezek, T. Collier and C. K. Brookner, *et al.* Laser scanning confocal microscopy of cervical tissue before and after application of acetic acid, *Am. J. Obstet. Gynecol.*, 2000, **182**(5), 1135–1139.

32 R. Samatham, S. L. Jacques Determine scattering coefficient and anisotropy of scattering of tissue phantoms using reflectance-mode confocal microscopy. In: *Proceedings of SPIE*. San Jose, CA, USA; 2009:718711–718711–8.

33 C. Bordier, C. Andraud and E. Charron, *et al.* Illustration of a bimodal system in Intralipid-20% by polarized light scattering: experiments and modeling, *Appl. Phys. A: Mater. Sci. Process.*, 2008, **94**(2), 347–355.

34 G. Born and M. Cross, The aggregation of blood platelets, *The Journal of physiology*, 1963, **168**(1), 178.

35 C. P. Markou, S. R. Hanson, J. M. Siegel, D. N. Ku The role of high wall shear rate of thrombus formation in stenoses. In: *Proc. ASME Biomed. Eng. Div.* New Orleans, LA; 1993.

36 B. Savage, J. J. Sixma and Z. M. Ruggeri, Functional self-association of von Willebrand factor during platelet adhesion under flow, *Proc. Natl. Acad. Sci. U. S. A.*, 2002, **99**(1), 425–430.

37 D. N. Ku and C. J. Flannery, Development of a flow-through system to create occluding thrombus, *Biorheology*, 2007, **44**(4), 273–284.

38 M. K. Runyon, B. L. Johnson-Kerner and R. F. Ismagilov, Minimal Functional Model of Hemostasis in a Biomimetic Microfluidic System, *Angew. Chem., Int. Ed.*, 2004, **43**(12), 1531–1536.

39 D. M. Wootton, A. S. Popel and B. R. Alevriadou, An experimental and theoretical study on the dissolution of mural fibrin clots by tissue-type plasminogen activator, *Biotechnol. Bioeng.*, 2002, **77**(4), 405–419.

40 D. N. Ku and D. Liepsch, The effects of non-Newtonian viscoelasticity and wall elasticity on flow at a 90 degrees bifurcation, *Biorheology*, 1986, **23**(4), 359–370.

41 D. A. Steinman and C. R. Ethier, The effect of wall distensibility on flow in a two-dimensional end-to-side anastomosis, *J. Biomech. Eng.*, 1994, **116**(3), 294.

42 D. Zeng, E. Boutsianis and M. Ammann, *et al.* A study on the compliance of a right coronary artery and its impact on wall shear stress, *J. Biomech. Eng.*, 2008, **130**(4), 041014–11.

43 M. H. Friedman, C. B. Bargeron, D. D. Duncan, G. M. Hutchins and F. F. Mark, Effects of arterial compliance and non-Newtonian rheology on correlations between intimal thickness and wall shear, *J. Biomech. Eng.*, 1992, **114**(3), 317–320.

44 D. Armani Re-configurable fluid circuits by PDMS elastomer micromachining. In: *IEEE International MEMS'99 Twelfth IEEE International Conference on Micro Electro Mechanical Systems*. Orlando, FL; 1999:222–227.

45 R. H. Peter, Physical properties of tissues relevant to arterial ultrasound imaging and blood velocity measurement, *Ultrasound Med. Biol.*, 2007, **33**(10), 1527–1539.

46 B. Gow and C. Hadfield, The elasticity of canine and human coronary arteries with reference to postmortem changes, *Circulation Research*, 1979, **45**(5), 588–594.

47 C. R. Ethier, C. A. Simmons *Introductory biomechanics: from cells to organisms*. 1st ed. Cambridge University Press; 2007.